Supplemental Information

A Therapeutic Antibody for Cancer, Derived from Single Human B Cells

Ryan T. Bushey, M. Anthony Moody, Nathan Nicely, Barton F. Haynes, S. Munir Alam, Stephen T. Keir, Rex C. Bentley, Kingshuk Roy Choudhury, Elizabeth B. Gottlin, Michael J. Campa, Hua-Xin Liao, and Edward F. Patz, Jr.

Table S1. Binding Kinetics of Human CFH mAbs as Determined by SPR

mAb	ka ($M^{-1}s^{-1}x10^{5}$)	kd ($s^{-1}x10^{-4}$)	Kd (nM)
7955	0.11	36.6	333
7957	1.95	8.61	4.42
7960	4.55	15.3	3.36
7964	2.18	10.5	4.82
7979	3.34	9.75	2.92
7961	1.96	7.83	3.99
7968	0.826	6.71	8.12

Related to Results: Isolation of Human CFH Antibodies from Patients with the Autoantibody

Table S2. Data Collection and Refinement Statistics for the Fab7968 - $CFH_{1110-1120}$ Structure

Data collection[a]	
Space group:	$P2_1$
Cell dimensions	
a, b, c (Å):	51.28, 65.55, 71.27
α, β, γ (°):	90.0, 106.4, 90.0
Resolution (Å)[b]:	38.0-2.0 (2.05-2.00)
R_{merge} (%):	8.2 (46.7)
<I/σ>	20.1 (3.2)
Completeness (%):	91.8 (100)[c]
Redundancy:	5.0 (5.1)
Refinement[c]	
Total # reflections:	26663 (1828)
Rwork / Rfree (%)	19.6 / 27.5 (24.8 / 37.5)
Wilson B ($Å^2$)	19.7
Nonhydrogen atoms	3721
Water molecules	341
R.M.S. deviations	
Bond lengths (Å):	0.009
Bond angles (°):	1.256
ψ, φ favored (%):	97.94
ψ, φ allowed (%):	1.38
ψ, φ outlying (%):	0.69

[a]*The crystal had one Fab-peptide complex in the asymmetric unit. The dataset came from a single crystal.*

[b]*Values in parentheses are for the highest resolution shells.*

[c]*Some mid-resolution shells suffered for completeness owing to high numbers of rejected reflections confounded by ice rings.*

Related to Figure 2

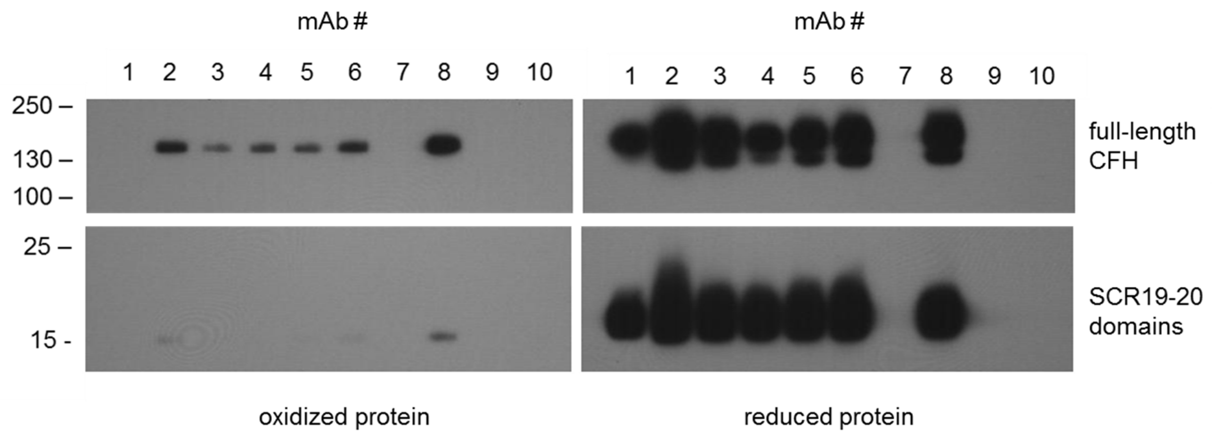

Figure S1. Immunoblot Analysis of 7 Recombinant CFH mAbs on Native and Reduced CFH and SCR19-20.

Related to Results: Isolation of Human CFH Antibodies from Patients with the Autoantibody

Equimolar amounts of CFH and SCR19-20 proteins (~150 kDa and ~15 kDa, respectively) were treated with Tris-HCl (oxidized) or TCEP (reduced) prior to being electrophoresed in the wells of a multi-chambered "Surf-Blot" apparatus. The proteins were transferred to PVDF, and immunoblots were reacted with recombinant CFH mAbs 1-6 and 8 or subtype-matched negative control mAbs 7, 9 and 10, loaded into individual wells. Binding was visualized with an anti-human IgG-HRP conjugate and chemiluminescent substrate, exposing the entire blot to one piece of film. (The relevant sections are shown.) Molecular mass markers are to the left, in kDa. Identity of CFH mAbs by well number: 1=7955; 2=7957; 3=7960; 4=7964; 5=7979; 6=7961; 8=7968.

residue mutated to A

mAb	P	I	D	N	G	D	I	T
7968	73	73	102	6	100	101	0	54
7955	52	8	81	0	104	103	0	1
7957	61	61	100	30	99	102	0	48
7960	53	43	95	0	99	99	0	4
7961	56	52	100	4	104	105	0	16
7964	74	76	100	35	100	102	0	66
7979	64	61	96	29	102	98	0	34
Ave	**62**	**54**	**96**	**15**	**101**	**101**	**0**	**32**

Consensus recognition sequence: PIDNGDIT

Figure S2. Alanine Scanning Mutagenesis: Binding of Human CFH mAbs to Alanine-Substituted Epitope Peptides.

Related to Figure 2

Biotinylated 15mer peptides, mutated in one of 8 positions (CFH1114-1121) to create alanine substitutions, were immobilized on streptavidin and binding of each of 7 antibodies to each peptide was determined by ELISA. Signal vs. antibody concentration curves were generated and the area under the curve was determined for each peptide-antibody pair. Each number in the figure represents the percent of antibody binding to the Ala-containing peptide vs. the naturally occurring peptide. Colors were overlaid by the "Conditional Formatting" function in Microsoft Excel using a gradient from highest (green) to lowest (red).

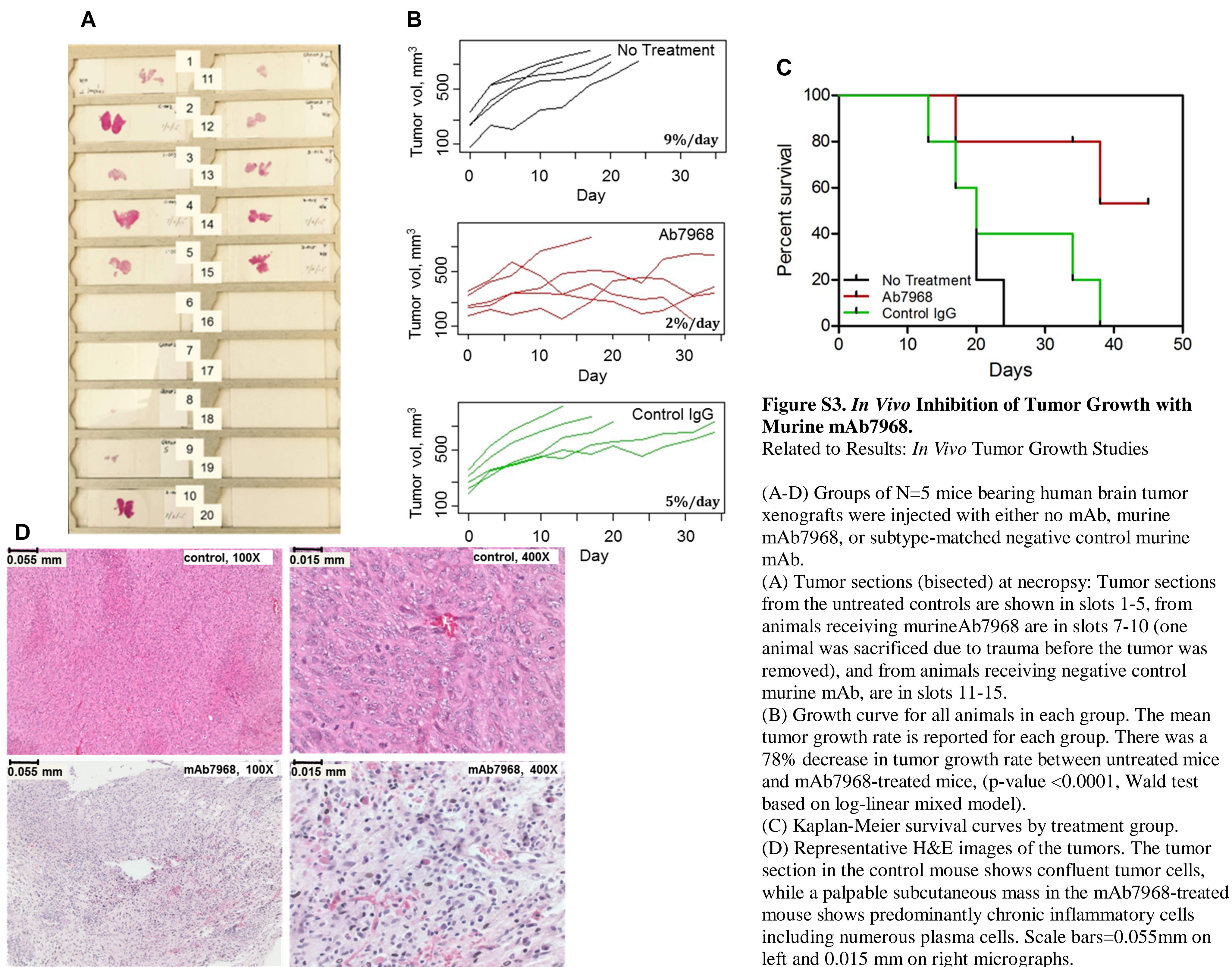

Figure S3. *In Vivo* Inhibition of Tumor Growth with Murine mAb7968.
Related to Results: *In Vivo* Tumor Growth Studies

(A-D) Groups of N=5 mice bearing human brain tumor xenografts were injected with either no mAb, murine mAb7968, or subtype-matched negative control murine mAb.
(A) Tumor sections (bisected) at necropsy: Tumor sections from the untreated controls are shown in slots 1-5, from animals receiving murineAb7968 are in slots 7-10 (one animal was sacrificed due to trauma before the tumor was removed), and from animals receiving negative control murine mAb, are in slots 11-15.
(B) Growth curve for all animals in each group. The mean tumor growth rate is reported for each group. There was a 78% decrease in tumor growth rate between untreated mice and mAb7968-treated mice, (p-value <0.0001, Wald test based on log-linear mixed model).
(C) Kaplan-Meier survival curves by treatment group.
(D) Representative H&E images of the tumors. The tumor section in the control mouse shows confluent tumor cells, while a palpable subcutaneous mass in the mAb7968-treated mouse shows predominantly chronic inflammatory cells including numerous plasma cells. Scale bars=0.055mm on left and 0.015 mm on right micrographs.

Supplemental Experimental Procedures

Affinity Measurement of Human CFH Antibodies by Surface Plasmon Resonance (SPR)

Antibody binding data, reported as dissociation constants (Kd) and rate constants (ka, kd), were obtained by SPR on a BIAcore 3000 instrument. Data analyses were performed using BIAevaluation 4.1 software (Biacore/GE Healthcare) as described earlier (Alam et al., 2011; Alam et al., 2008). Epitope-containing 15mer peptide or a scrambled 15mer peptide, each with a biotin tag, were coupled to individual flow cells of a streptavidin coated chip at 60 and 14 response units (RU) respectively. Antibodies were injected at 50 μl/min for a 5 min association time at concentrations of 0.1, 0.2. 0.5 and 1.0 μg/ml. Antibody bound surfaces were regenerated after each cycle with a pulse of glycine pH2.0 buffer. Rate constants were derived by global curve fitting analysis to a Langmuir 1:1 model of specific antibody binding responses following subtraction of non-specific signal on the scrambled control peptide surface.

Epitope Mapping of Human CFH mAbs by ELISA

Binding of recombinant CFH mAbs to wild type epitope-peptide and variants with single alanine substitutions was measured by ELISA using the following procedure: 384-well high binding plates (Costar #3700) were coated with 2 μg/ml streptavidin (Life Technologies) at 30 ng/well in 0.1 M sodium bicarbonate and incubated overnight at 4 °C. The next day, wells were blocked for 1 hour with assay diluent (PBS containing 4% (w/v) whey protein, 15% normal goat serum, 0.5% Tween-20, 0.05% sodium azide) at 40 μl/well. Plates were then washed once with 1X PBS, 0.1% Tween-20 solution and incubated for 25-30 minutes with biotinylated peptides diluted to 2 μg/ml in assay diluent (10 μl/well). The plates were then washed once, and purified IgG antibodies were added starting at 100 μg/ml with 3-fold dilution at 10 μl/well and incubated for 1

hour at room temperature. Following two washes, an IgG goat-anti-human Fc specific HRP conjugated secondary antibody (Rockland) was diluted in assay diluent without sodium azide at 1:10,000 and added at 10 µl/well and incubated for 1 hour. To develop, plates were washed four times and binding was detected with 20 µl/well of SureBlue Reserve (KPL) for 15 minutes. Reaction was stopped with the addition of 20 µl/well 0.33 N HCl. Absorbance was determined at 450 nm using a Spectromax 384plus plate reader (Molecular Devices).

In Vivo Tumor Growth Study: D-270MG Brain Cancer Model in the Nude Mouse

Animal care was in accordance with Duke University IACUC guidelines. As described in the text, for *in vivo* mouse studies we developed a mAb7968 chimeric antibody that contained the VH and VK region genes of Ab7968 and the constant region of mouse IgG1 (Strausberg et al., 2002) and mouse Ig kappa light chain (Svasti and Milstein, 1972). To test the effect of antibody on tumor growth, we used an adult patient-derived brain tumor xenograft, D-270MG, grown in nude mice (Bigner et al., 1990). After allowing tumors to grow to approximately 150-250 mm^3 in volume we performed intratumoral injections (200 µg) of murine IgG1-mAb7968, murine subtype-matched negative control mAb, or no antibody. Injections were repeated biweekly for 3 weeks. The study personnel administering the drugs and measuring the tumors were blinded. Tumors were measured biweekly and animals were sacrificed when the tumors grew beyond 5 times the initial size (tested-out). Tumors removed at necropsy were fixed in 10% formalin and embedded in paraffin. Five micron thick sections were stained with hematoxylin and eosin (H&E) for histologic evaluation.

Statistical Evaluation of Tumor Growth in the Nude Mouse

Given that growth appears approximately log linear for all treatment groups, we fit a model of the form:

$$\log\left(V_{ij}\left(t\right)\right) = \alpha_c + \alpha_j + a_{ij} + \beta_c t + \beta_j t + \varepsilon_{ijt}$$

Where $V_{\mathrm{ij}}(t)$ is tumor size for the i-th animal ($i = 1,2,\ldots,5$) in the j-th group ($\mathrm{j} = 1,\ldots,5$) at timepoint t. The model explains this in terms of a mean initial volume $\alpha_{\mathrm{c}} + \alpha_{\mathrm{j}}$ in the j-th group, an animal specific initial volume a_{ij}, assumed to be random, with a zero mean Gaussian distribution, b_c a rate of growth in the control group and b_j, the difference in growth rate between treatment j and the control growth rate. The model was fit by restricted maximum likelihood using the **nlme** package in the R computing platform (www.r-project.org). Hypothesis tests for growth rate inhibition were based on Wald tests using parameter estimates and standard errors from this model.

References (not otherwise cited in the text)

Alam, S.M., Liao, H.X., Dennison, S.M., Jaeger, F., Parks, R., Anasti, K., Foulger, A., Donathan, M., Lucas, J., Verkoczy, L., *et al.* (2011). Differential reactivity of germ line allelic variants of a broadly neutralizing HIV-1 antibody to a gp41 fusion intermediate conformation. J Virol *85*, 11725-11731.

Alam, S.M., Scearce, R.M., Parks, R.J., Plonk, K., Plonk, S.G., Sutherland, L.L., Gorny, M.K., Zolla-Pazner, S., Vanleeuwen, S., Moody, M.A., *et al.* (2008). Human immunodeficiency virus type 1 gp41 antibodies that mask membrane proximal region epitopes: antibody binding kinetics, induction, and potential for regulation in acute infection. J Virol *82*, 115-125.